

Current-induced local oxidation of metal films: Mechanism and quantum-size effects

Thomas Schmidt, Richard Martel, Robert L. Sandstrom, and Phaedon Avouris^{a)}
IBM Research Division, T. J. Watson Research Center, Yorktown Heights, New York 10598

(Received 23 June 1998; accepted for publication 11 August 1998)

A novel route is introduced for oxidizing thin metal films with nanometer-scale resolution. By locally subjecting Ti and Nb films to high in-plane current densities, metal-oxide tunneling barriers are formed in a self-limiting fashion. The oxidation is triggered by current-induced atomic rearrangements and local heating. At the final stages of the barrier formation, when only atomic-scale channels remain unoxidized, the oxidation rate decreases drastically while the conductance drops in steps of about $2e^2/h$. This behavior gives evidence of ballistic transport and a superior stability of such metallic nanowires against current-induced forces compared with the bulk metal. © 1998 American Institute of Physics. [S0003-6951(98)04741-X]

One of the driving forces for modifying materials on the nanometer scale is the desire to explore novel quantum transport phenomena. Thus, techniques that allow the controlled formation of nanometer-scale tunneling barriers become increasingly important. An interesting approach is to utilize the tip of an atomic force microscope (AFM) to define oxide barriers in metal films.^{1,2} This electrochemical anodization process is induced by biasing the tip to generate an electric field perpendicular to the metal surface.³

In this letter, we show that high in-plane current densities can be employed to locally oxidize thin conductors under ambient conditions. This *current-induced local oxidation* (CILO) process allows us to form metal-insulator-metal tunneling diodes with nanometer-scale barriers in a self-limiting fashion. Towards the end of the barrier formation, the conductance of the film decreases in steps of about $2e^2/h$, which we discuss in terms of conductance quantization in atomic-scale metallic wires formed during the CILO experiment.

For our experiments, we prepared thin Ti and Nb strips such as the one shown in the AFM image Fig. 1(a). In this case, a 4-nm-thick Ti film was evaporated on a SiO₂ layer thermally grown on a Si(100) wafer. The Ti layer is polycrystalline with a grain size of about 3 nm, a surface roughness of 0.5 nm, and a sheet resistance of $R_{\square} = 2 \text{ k}\Omega$. Optical lithography was used to pattern the Ti film into 1 to 2- μm -wide strips connected to Au/Al contact pads. In order to locally constrict the Ti strips, TiO_x notches were defined by employing the AFM tip-induced oxidation process [clearly visible in Fig. 1(b)].¹⁻³ The oxide protrudes from the surface reflecting the volume expansion upon oxidation.⁴

Metal strips with 100–200-nm-wide constrictions and a film resistance of $R_F \approx 10 \text{ k}\Omega$ are the starting point for our study. Upon biasing the structure shown in Fig. 1(b) with a constant stress voltage of $V = 2 \text{ V}$, we measured an initial current flow of $I = 200 \mu\text{A}$ across the Ti strip, corresponding to a current density of $j \approx 10^7 \text{ A/cm}^2$ inside the constriction. However, the current started to decrease immediately, stabi-

lizing a few minutes later at a two orders of magnitude lower value. Figure 1(c) shows that, in the meantime, the gap has been closed by a newly formed 20-nm-wide barrier. This barrier protrudes by 1.5 nm from the Ti surface, which is close to the value for the AFM-tip induced oxide.

Current–voltage (I – V) curves obtained before applying the stress voltage were linear but, as can be seen in Fig. 1(d), they became highly nonlinear after the barrier had been formed. Such nonlinear I – V curves are characteristic of metal-insulator-metal diodes, in which both tunneling through the barrier and thermionic emission contribute to the current.⁵ To determine the barrier height from the thermionic emission, we measured the temperature dependence of the I – V curve of a 50-nm-wide barrier formed at a stress voltage of 5 V so as to suppress tunneling. From the slope of $\ln I$ vs $1/T$ curves constructed from the I – V data of Fig. 1(e), we obtained a barrier height of $\phi_0 = 0.24 \text{ eV}$. This value is close to the upper limit of the range of 0.1–0.3 eV previously reported for TiO_x barriers.⁶

Both the barrier height ϕ_0 and the volume expansion suggest that the barrier results from local oxidation. To support this conclusion, we tried to repeat the experiment in a He atmosphere, where, indeed, no barrier formation could be observed. We note that the current-induced oxidation occurs under conditions entirely different from the AFM tip-induced oxidation. In the latter case, the oxidation is induced by high electric fields of 10^7 V/cm oriented perpendicular to the surface, which drive the oxidant into the film.³ In contrast, the stress voltage during the CILO process leads to electric fields of 10^5 V/cm , which are not only orders of magnitude lower but also oriented in the plane of the film.

To study the mechanism of the CILO process, we interrupted the oxidation and imaged the barrier growth with the AFM. The oxide barrier extends uniformly across the entire gap even at the initial stages of CILO, which indicates that the oxide grows from the Ti surface down towards the Ti/SiO₂ interface.

The time evolution of the conductance (G – t) upon application of the stress voltage provides a measure of the rate of the barrier formation. As shown in Fig. 1(f), initially the conductance of the film decreases slowly but it drops in-

^{a)}Electronic mail: avouris@us.ibm.com

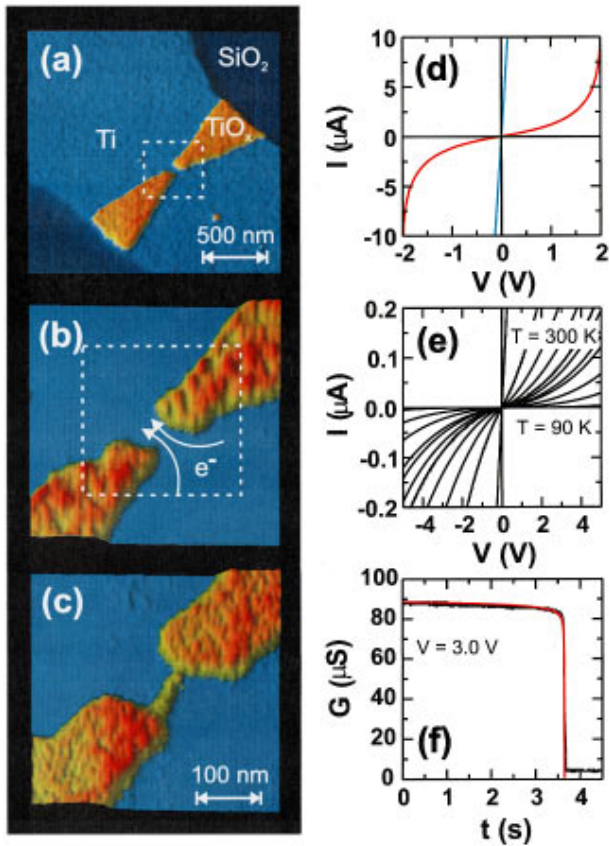


FIG. 1. (a) AFM image of a 4-nm-thick Ti strip on SiO_2 with a TiO_x constriction in the center. (b) Close up view of the gap region. (c) AFM image after the gap has been closed by a 20-nm-wide barrier upon applying a stress voltage of 2 V. (d) I - V curves of the device before (blue) and after the barrier formation (red). (e) Temperature dependent I - V data from a device stressed at $V=5$ V. (f) Time evolution of the conductance during CILO (black) compared with a simulation of the oxidation (red).

creasingly faster as CILO proceeds. This behavior indicates that the rate strongly depends on the current density j , since, as the barrier grows, the cross sectional area S of the metallic path through the constriction decreases. It is useful to split the total film resistance into $R=R_L+R_G$, with R_L being the constant resistance of the macroscopic leads and $R_G\propto 1/S$ the resistance of the gap region. Initially, R is dominated by the lead resistance R_L , which exceeds R_G by 1 to 2 orders of magnitude. Hence, S shrinks much faster during CILO than R grows, such that the local current density $j=V/SR$ inside the gap increases strongly (R_G dominates R only after S decreased by $>95\%$). By writing the oxidation rate as $dS/dt=-\text{const}\times j^n$, we simulated the G - t curve and obtained an exponent of $n=4$ [Fig. 1(f)]. The local character of the oxidation results from this superlinear dependence on the current density, which confines the barrier formation to the part of the constriction where j is maximal.

To develop a microscopic model for the CILO process, we note that current densities of $j\geq 10^6$ A/cm² produce forces on atomic defects in metals which lead to macroscopic material transport—a phenomenon known as electromigration.⁷ The dominant force is the electron wind force which results from momentum transfer to defect atoms due to electron scattering. It can be estimated as $F_{ew}\sim 2mv_F(js/e)$, with s being the scattering cross section and e , m , and v_F the charge, mass, and Fermi velocity of the

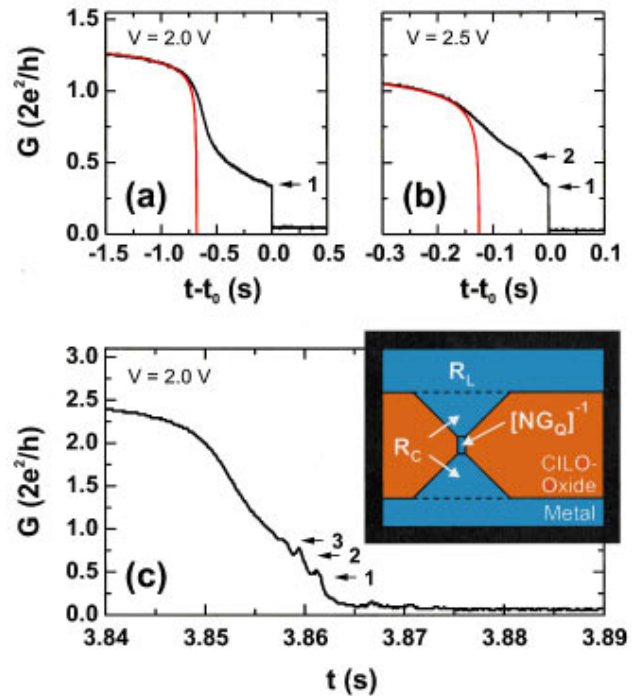


FIG. 2. (a) and (b) G - t curves recorded during the final stages of CILO experiments on Ti (black) in comparison with the CILO simulation (red). (c) G - t curve of a CILO experiment on Nb. The inset shows a scheme of a metallic nanowire formed during the CILO process.

electrons. At $j=10^6$ A/cm², the wind force $F_{ew}\sim 10^{-5}$ nN is by orders of magnitude too small to break atomic bonds. However, current-induced forces enhance diffusion and make it directional, such that atom and vacancy flux densities $j_{a,v}\propto Dj$ are generated, with D being the atomic diffusion coefficient. Thus, nanocracks are formed preferentially at grain boundaries, which further increases the current density in the undamaged film regions and eventually destroys the conductor on a macroscopic scale. At $j>10^8$ A/cm², we observe the instantaneous destruction of our Ti film associated with the formation of macroscopic voids and hillocks characteristic of electromigration. The CILO process is triggered by current densities of $j\approx 10^7$ A/cm², which are well in the range where atomic rearrangements occur. Hence, we propose that CILO involves initial stages of electromigration, i.e., the opening of the grain boundaries of the metal film, which act as channels for the transport of the oxidant from the surface to the bulk of the conductor. As atomic rearrangements scale linearly with j , the observed j^4 dependence of the barrier-formation rate suggests that local heating is important as well. From a simulation of energy dissipation and heat conduction in the Ti strips, we estimate the film temperature inside the gap to reach $T\sim 1000$ K. Apart from Joule heating, localized vibrational excitations of defects may also play an important role.^{8,9} Local heating facilitates atomic motion due to the exponential temperature dependence of the diffusion coefficient and activates the oxidation.¹⁰

An interesting feature of the CILO process is its self-limiting character. After the completion of the barrier, the current density is by orders of magnitude lower than before and the oxidation stops. If desired, the barrier width can be further increased by raising the stress voltage.

Considering in more detail the time dependence of CILO, we find striking deviations from the simple $dS/dt = -\text{const} \times j^4$ behavior towards the end of the barrier formation. Figure 2(a) shows that the decrease of the conductance in time slows down, which reflects a *reduction of the oxidation rate*. Finally, a sharp step signifies the completion of the barrier. The magnitude of this step is of the order of the conductance quantum $2e^2/h$, but its exact value depends on the initial resistance R_F of the open constriction. By performing a large number of CILO experiments, we found that the step magnitude is larger, the smaller R_F has been before the oxidation. Figure 2(b) shows additional fine structure reminiscent of a second step. The geometry of our strips defines a lower limit of $R_F \approx 5R_{\square}$ for their resistance. To reduce the sheet resistance R_{\square} , we used a 4-nm-thick Nb film for the CILO process and observed three clear steps in the $G-t$ curve [Fig. 2(c)].

To reveal the origin of these conductance steps, we note that the metallic path in the constriction shrinks continuously as the oxide barrier grows. Eventually, only an atomic-scale channel with lateral dimensions of the order of the Fermi wavelength remains unoxidized. Such a metallic nanowire has laterally quantized modes (energy levels) and its conductance is given by the Landauer formula $G = G_Q \sum_{i=1}^N T_i$, with N being the number of occupied modes, T_i the transmission coefficient of mode i , and $G_Q = 2e^2/h$ the conductance quantum.¹¹ As the cross section of the nanowire shrinks due to oxidation, the number of occupied modes decreases, which explains the stepwise reduction of the conductance at the final stages of CILO. Previously, steps of the order of $2e^2/h$ have been observed in many experiments^{12,13} mostly involving the mechanical elongation of atomic-scale metallic junctions.

In the case of the CILO experiment, we find clear evidence that ballistic effects play an important role. The conductance steps are accompanied by a decreasing oxidation rate, which signifies an enhanced stability of the nanowire against current-induced oxidation compared with the bulk film. This is even more surprising taking into account that the current density in the nanowire reaches $j \sim 10^{11}$ A/cm². Under such conditions, an electron wind force of $F_{ew} \sim 1$ nN comparable to the atomic binding forces acts on defects. The high stability of the nanowire shows that electron-defect scattering and energy relaxation are locally strongly suppressed, which implies that the wire is essentially defect free and therefore exhibits ballistic transport. In fact, our nanowires are most likely to be formed in film regions with perfect crystalline order, because CILO, driven by electromigration and local heating, proceeds faster where the defect density in the metal is higher.

For a more quantitative analysis, we note that the conductance was measured at the high stress voltage required for the oxidation, which prevents the observation of a larger number of conductance steps.¹⁴ Moreover, a considerable lead resistance R_S is connected in series to the nanowire, which reduces the step magnitude. In Fig. 2(c), steps occur at $G_3 = 0.9G_Q$, $G_2 = 0.75G_Q$, and $G_1 = 0.5G_Q$. Assuming $T_i \sim 1$ in Landauer's formula, we evaluate the series resistance from $[G_N]^{-1} = [NG_Q]^{-1} + R_{S,N}$ and obtain $R_{S,3} = 10$ k Ω , $R_{S,2} = 11$ k Ω , and $R_{S,1} = 13$ k Ω . These values exceed the re-

sistance $R_F = 4.5$ k Ω of the open constriction, which may be related to microscopic channels that connect the nanowire to the macroscopic leads of resistance $R_L \approx R_F$ [see inset of Fig. 2(c)]. Since transport in these channels remains essentially diffusive, CILO tends to increase their resistance R_C , such that the total series resistance $R_S \approx R_L + R_C$ increases as the number of occupied modes in the nanowire decreases. Although we cannot rule out deviations from unit transmission, the sizeable series resistance explains why the step magnitude in different CILO experiments is larger, the smaller R_F has been before the oxidation.

In conclusion, we discovered that thin metal films can be oxidized by high in-plane current densities. This novel oxidation process involves initial stages of electromigration and local heating and allows the formation of metal-oxide tunneling barriers with nanometer-scale resolution. Towards the end of the barrier formation, only atomic-scale channels remain unoxidized. Despite a strongly increased current density, the oxidation rate decreases drastically and the conductance drops in steps of about $2e^2/h$. This gives evidence of ballistic transport and a superior stability of such metallic nanowires against current-induced forces compared with the bulk metal, which may be of great importance for future atomic-scale electronic devices. It is likely that other chemical reactions, for example, nitride barrier formation from reaction with NH_3 , can be induced by high current densities as well.

We thank H. R. Shea and B. Ek for experimental assistance and T. Hertel, R. Landauer, and N. Lang for discussions.

¹ See, e.g., J. A. Dagata, *Science* **270**, 1625 (1995), and references therein.

² E. S. Snow and P. M. Campbell, *Science* **270**, 1639 (1995).

³ Ph. Avouris, T. Hertel, and R. Martel, *Appl. Phys. Lett.* **71**, 285 (1997).

⁴ Oxidation of Ti to TiO_2 involves a volume expansion by a factor of 1.6.

⁵ S. M. Sze, *Physics of Semiconductor Devices* (Wiley, New York, 1981).

⁶ K. Matsumoto, M. Ishii, K. Segawa, Y. Oka, B. J. Vartanian, and J. S. Harris, *Jpn. J. Appl. Phys., Part 1* **34**, 1387 (1995); E. S. Snow, P. M. Campbell, and D. Park, *Superlattices Microstruct.* **20**, 545 (1996); B. Imer, M. Kehrlé, H. Lorenz, and J. P. Kotthaus, *Appl. Phys. Lett.* **71**, 1733 (1997).

⁷ See, e.g., *Electromigration & Electronic Device Degradation*, edited by A. Christou (Wiley, New York, 1994).

⁸ K. S. Ralls, D. C. Ralph, and R. A. Buhrman, *Phys. Rev. B* **40**, 11 561 (1989).

⁹ R. S. Sorbello, *Mater. Res. Soc. Symp. Proc.* **427**, 73 (1996); R. E. Walkup, D. M. News, and Ph. Avouris, *Phys. Rev. B* **48**, 1858 (1993).

¹⁰ Local heating favors complete oxidation to TiO_2 . This is perhaps the reason why the CILO barrier height is at the upper limit of the range reported for TiO_x (also exceeding the 0.14 eV of our AFM tip-induced oxide).⁶

¹¹ R. Landauer, *J. Phys.: Condens. Matter* **1**, 8099 (1989).

¹² See, for example, J. I. Pascual, J. Méndez, J. Gómez-Herrero, A. M. Baró, N. García, U. Landman, W. D. Luedtke, E. N. Bogachek, and H.-P. Cheng, *Science* **267**, 1793 (1995); J. M. Krans, J. M. van Ruitenbeek, V. V. Fisun, I. K. Yanson, and L. J. de Jongh, *Nature (London)* **375**, 767 (1995); E. S. Snow, D. Park, and P. M. Campbell, *Appl. Phys. Lett.* **69**, 269 (1996); E. Scheer, P. Joyez, D. Esteve, C. Urbina, and M. H. Devoret, *Phys. Rev. Lett.* **78**, 3535 (1997).

¹³ See also *Nanowires*, edited by P. A. Serena and N. García (Kluwer Academic, Dordrecht, 1997).

¹⁴ L. I. Glazman and A. V. Khaetskii, *Europhys. Lett.* **9**, 263 (1989); H. Yasuda and A. Sakai, *Phys. Rev. B* **56**, 1069 (1997).